STATIC AND DYNAMIC BEHAVIOR OF A 3D-PERIODIC STRUCTURE

J. Rishmany, L. Renault, C. Mabru, R. Chieragatti, F. Rezaï Aria *
Ecole Nationale Supérieure d'Ingénieurs de Constructions Aéronautiques
1, Place Emile Blouin, 31056 Toulouse, France
* Ecole des Mines d'Albi-Carmaux
Route de Teillet, 81013 Albi, France
rjihad@ensica.fr

ABSTRACT

This contribution deals with the assessment of static and dynamic behavior a 3D-periodic structure. Equivalent Young and shear moduli are evaluated respectively via a spring-network calculation performed on a representative volume element (RVE) of the structure and an energy approach. To assess the accuracy of the two methods, FE simulations are performed, and tensile experiments are conducted on specimens cut out from 3D-structure panels. Results show disagreement for stiffness values along y-direction. This is thought to be due to stiffness variation between RVE's due to boundary conditions. A new analytical/numerical approach is proposed taking into consideration the presence of different types of boundary conditions on RVE's. Static results are further used as an input for FE investigations of the dynamic behavior of the structure. Two models are proposed: a) homogeneous and b) laminated models. Vibration tests are performed on different specimens and fundamental frequencies are noted. Results for both models correlate well with experimental data. However, the homogeneous model is limited to low frequencies.

Introduction

The equipment concerned in this study is the core of an air-to-air compact heat exchanger. It consists of a block of alternating layers (passages) of fins. The layers are separated from each other by parting sheets and sealed along the edges by means of closure bars, and are provided with inlet and outlet ports for the streams. End sheets at the top and bottom bound the block. The stacked assembly is brazed in a vacuum furnace to become a rigid core.
Heat exchangers are subjected in service to pressure, temperature and vibration, thus creating a complex loading and environment that renders difficult the prediction of their lifetime. Testing of such equipments under real service conditions is a very expensive and time-consuming process. An alternative solution is to perform accelerated tests requiring a prior understanding of the static and dynamic behavior of the equipment, in particular the core behavior. These two goals constitute our main interest in this study.
The main purpose is to find out an equivalent stiffness matrix for the exchanger core. The core constitutes a periodic structure with 2 repetitive plies at 0 and 90 ° respectively (Figure-1). Each ply is constituted of fins that are bounded by two half-plates, thus forming a 3D-wavy-sandwich structure. Several models dealing with the assessment of the behavior of such structures are reported in literature:

- Models based on the classical laminate theory (CLT) [1-3], which are widely used in literature for wavy structures. However, these models present shortcoming for predictions of transverse moduli, E_{33}, and G_{13}. Therefore, this approach does not allow determining all the elements of the stiffness matrix of the core, and thus no finite element calculations would further be possible to assess the dynamic behavior of the core.
- Analytical/numerical models [4], where the average stiffness properties are first calculated by the effective-modulus theory. Theses average stiffness properties are given as an input for computing the elemental stiffness matrix in the finite element formulation.
- Strain energy based Representative Volume element (RVE) concept [5-6], which assumes equivalence of the mechanical behavior of RVE for the given structure and a similar volume element consisting of the effective medium, if equal strain energy in both volume elements is caused by strain states that are equal in a volume average sense.

In this study, Young's moduli are computed via a spring network calculation performed on a RVE of the core, assuming either isostress or isostrain conditions along each direction. First, average stiffness values are found and then, Young's moduli are evaluated via a homogenization technique. Shear moduli are found via an energy-based approach combined with mechanics

of materials where every ply is modeled separately. A 2D-unit cell is defined for each ply, and lower and upper bounds for equivalent shear stiffness are evaluated. However, only 2 shear moduli can be bounded: G_{12} and G_{23}. The third modulus is only found via finite element calculation.

Core geometry

As mentioned earlier, the core of the exchanger consists of a block of alternating layers of fins. Figure 1 shows a sketch presentation of the core.

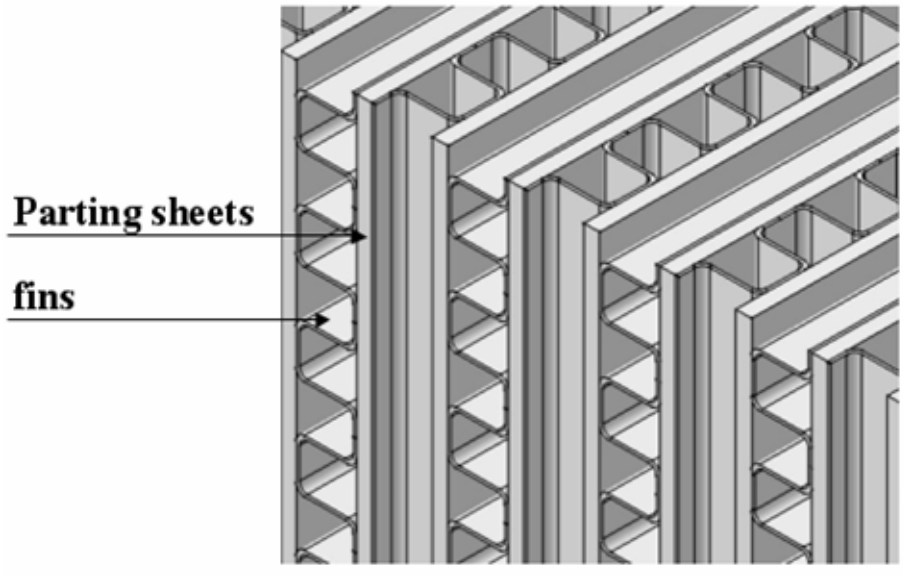

Figure 1. A schematic presentation of the core of a heat exchanger

The sheets and the fins are made of two isotropic materials with similar physical properties E, ν and G, with

$$G = \frac{E}{2(1+\nu)} \tag{1}$$

where E, ν and G are respectively, the Young's modulus, the Poisson's ratio, and the shear modulus.
Moreover, like sandwich structures, the core is supposed to have an orthotropic behavior. Poisson's ratios are also neglected. The numerical FEM calculations have shown that the latter assumption is relevant. Hereafter, analytical formulations for estimation of the equivalent Young's and shear moduli are presented.

Formulation of equivalent Young's moduli

In order to evaluate the average stiffness of the core, an approximate spring calculation is conducted at two levels: 1) the average local stiffness of the RVE is found, and 2) the global average stiffness of the structure (core level) is found. Figure 2 presents the RVE of the core. It consists of two alternating fins separated by a sheet and bounded at the top and the bottom by two half-sheets. The 3D-structure of the core can be formed by assembling several RVE's in all three directions.

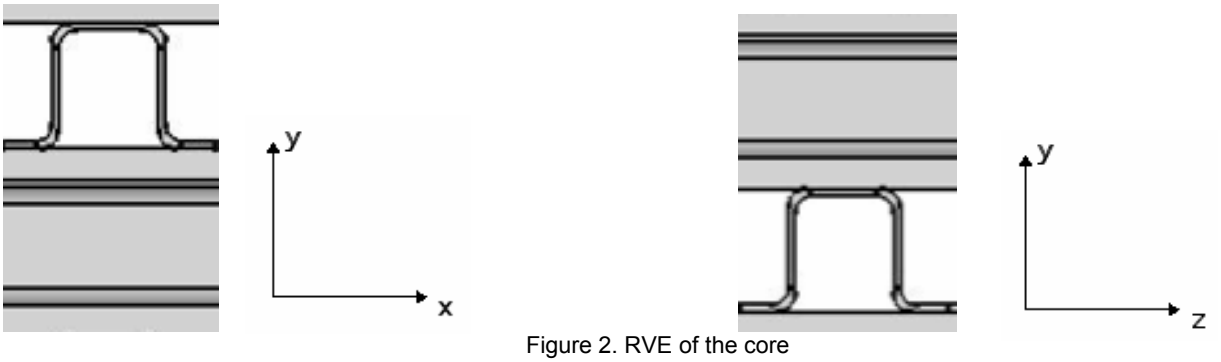

Figure 2. RVE of the core

The average stiffness of the RVE is found by dividing the RVE into (n) substructures, each having a stiffness (k_i) and replacing these substructures by a spring network [7], with n the number of substructures and k_i the stiffness of the i^{th} substructure. Hence, finding the stiffness of the RVE is reduced to calculate the equivalent stiffness of the spring network.
Moreover, in order to simplify the calculations, the following assumptions are made:

- Brazing in neglected in calculation,
- The material has a linear-elastic behavior,
- Perfect bonding exists between the fins and the sheets,
- Along (x) and (z) directions, deformation of the RVE is mainly due to the deformation of the plates and the longitudinal fins, hence the stiffness of transversal fins is neglected along these 2 directions.

Beam theory is used to find the stiffness of substructures. Once the stiffness of RVE is calculated, a spring network at the core level is considered and the stiffness of the core as well as that of different specimens is found. The stiffness of specimen is calculated in the extensometer zone in order to compare the analytical and the experimental results. Equivalent Young's moduli can be easily obtained from the average stiffness properties by homogenization. For a beam, the equivalent Young's modulus along x-axis would be:

$$E_{x,\mathrm{hom}} = \frac{K_x . l_x}{S_{x,\mathrm{hom}}} \tag{2}$$

where, $E_{x,hom}$, K_x, l_x, and $S_{x,hom}$ are respectively the equivalent Young's modulus, the average stiffness of the structure, the length of the structure, and the equivalent surface of the structure having as normal the x-axis.
The equivalent Young's moduli along (y) and (z) axes are found in a similar manner.

Formulation of equivalent core shear moduli G^e_{xz} and G^e_{yz}

Unlike the cases of Young's moduli, the shear stiffness usually involves a complicated state of deformation, and it is relatively difficult to get an exact analytical solution. However, using the energy approach, the lower and upper bound solutions can be obtained [3]. The energy theory states that the strain energy calculated from the exact displacement distribution is a minimum. For a given simplified sandwich core, the averaging principle of RVE technique can be generally expressed in parallel and series models according to Voigt and Reuss:

$$\frac{1}{2}\frac{\sigma_{ij}^2}{C_{ij}} V \le \sum_{k=1}^{n} (U_b + U_s + U_a)_k \tag{3}$$

$$\frac{1}{2} C_{ij} \varepsilon_{ij}^2 V \le \sum_{k=1}^{n} (U_b + U_s + U_a)_k \tag{4}$$

where k accounts for individual substructures in the RVE, and U_b, U_s, and U_a are respectively the bending, shear, and axial strain energies.

The difficulty is mainly due to the alternation of the two layers of fins forming the RVE where the form of the cross-section depends on the position of the cut. To overcome this problem, the core is simplified and considered as a laminate composed of two repetitive alternating layers. Therefore, two new unit cells are considered each representing a layer, and the calculation is performed on each unit cell separately (figure 3-a). To simplify calculation, an equivalent structure is considered (figure 3-b) where fillets are replaced by straight lines.

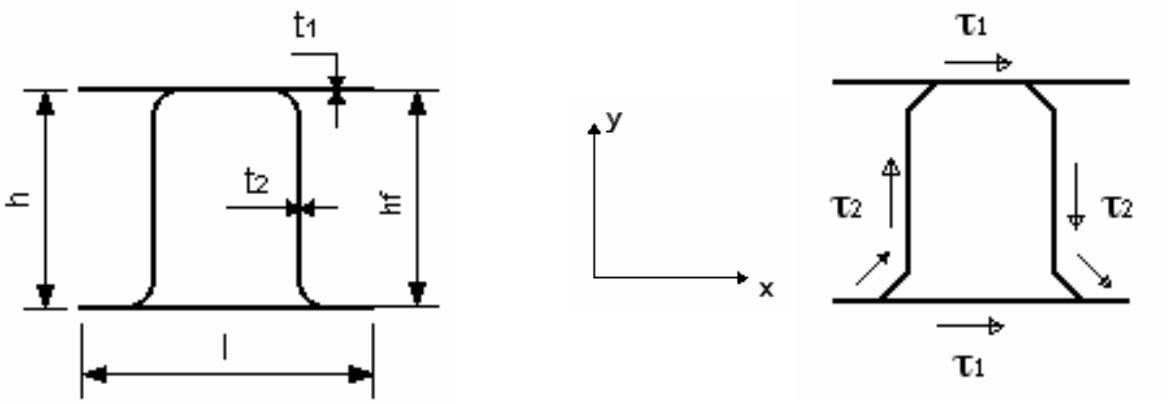

Figure 3. (a) Unit cell representing a layer (b) Simplified unit cell

When a shear stress τ_{xz} is applied along the x-direction, the resulting apparent distributed shear flow is as shown in figure 3-b. The equilibrium equation and compatibility requirements are written as:

$$2t_2 \int_0^s \tau_2 \cos\vartheta ds + 2t_1 l \tau_1 = hl\tau_{xz} \tag{5}$$

$$2\int_0^s \frac{\tau_2}{G} ds = \frac{\tau_2}{G} l \tag{6}$$

where G is the shear modulus of the constitutive material of the core, and θ is the angle between the fin and the x-axis (θ is constant in every portion of the fin), with

$$2\int_0^s \cos\vartheta ds = l \tag{7}$$

Equations (5) and (6) lead to:

$$\tau_1 = \frac{2h\int_0^s ds}{lt_2 + 4t_1 \int_0^s ds}\tau_{xz} \tag{8}$$

and

$$\tau_2 = \frac{lh}{lt_2 + 4t_1 \int_0^s ds}\tau_{xz} \tag{9}$$

By applying equation (3), we obtain:

$$\frac{G_{xz}^e}{G} \geq \frac{lt_2}{2h\int_0^s ds} + \frac{2t_1}{h} \tag{10}$$

Similarly, applying a shear strain ε_{xz} and considering the corresponding compatibility conditions, equation (4) becomes:

$$lhG_{xz}^e \varepsilon_{xz}^2 \leq 2t_1 lG\varepsilon_{xz}^2 + 2t_2 G\varepsilon_{xz}^2 \int_0^s \cos^2\vartheta ds \tag{11}$$

Simplifying equation (11), we obtain:

$$\frac{G_{xz}^e}{G} \leq \frac{2G}{lh}(t_1 l + t_2 \int_0^s \cos^2\vartheta ds) \tag{12}$$

Following a similar analysis process, the core shear modulus, G^e_{yz}, can be obtained as:

$$\frac{2t_2 h_f^2}{hl\int_0^s ds} G \leq G_{yz}^e \leq \frac{2t_2 \int_0^s \sin^2\theta ds}{lh} G \tag{13}$$

Experimental procedures and specimen preparation

To assess the accuracy of the analytical method proposed for the evaluation of the equivalent Young's moduli, tensile tests were conducted along two directions (y) and (z) on specimens cut out from the core. Results along x-axis could be obtained from those along z-axis by analogy. Also vibration tests were conducted on specimens using the impulse-response (IR) technique to determine the dynamic behavior of the core.

For tensile tests along z-axis, the two ends of the specimens were filled with resin to better distribute the clamping force and to limit stress concentrations. Reinforcing plates were also glued at both ends (figure-4a, post-experiment photo) using a bi-component adhesive. Two extensometers were mounted on the specimens for displacement measurement.
For tensile tests along y-axis, shoulders were glued on both ends of the specimens (figure-4b). One or more extensometers were mounted on the specimens according to their length.

(a) (b)

Figure 4. Specimen for tensile test along (a) z-axis (b) y-axis

Test conditions

Tensile tests were conducted at room temperature. Two types of loadings were applied:

- Rupture tensile testing with no loading/unloading with a displacement rate of 0.5 mm/min.
- Rupture tensile testing with several loading/unloading.

For dynamic testing, the impulse-response (IR) technique was used, which is a non-destructive sonic method generally used to determine the dynamic properties (frequencies, damping ratios and mode shapes) of structural systems. The technique consists principally of two stages; striking the specimen with a mechanical device such as a hammer and then monitoring the response by attaching a transducer to the specimen. The impact (force) produced by the mechanical device during a short transient period induces stress waves, which reflect back and forth within the structural system between boundary interfaces until the mechanically induced energy is consumed by material damping, dispersion and reflections. For our tests, specimens were hung freely using rubber elastics. A piezo-electric accelerometer was attached to the specimen using wax, and an instrumented hammer, equipped with a force transducer to capture the induced force, was used to strike the specimen (figure-5). Signals from the instrumented hammer and accelerometer were fed into a 2-channel frequency analyzer with signal storage capabilities. Results were then post-treated using Proview. Fast Fourier Transforms (FFT) of specimen response were obtained from signal vs time graphs using Famos. Numerous spectral peaks, which correspond to the resonant frequencies of the specimen, can be readily identified.

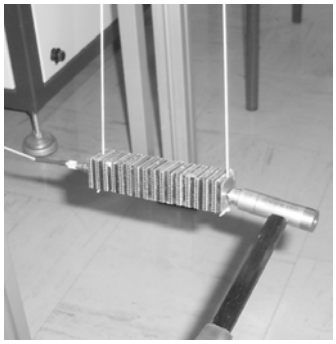

Figure 5. Dynamic testing of specimen using IR technique

Experimental results

Charge-Deformation diagrams were plotted for tensile tests (Figure-6). Examination of the results along y-axis show that the charge-deformation curve is formed of 3 parts:

- The first part, with a variable slope depending on the initial form of fins,
- The second part with a constant slope representing the apparent stiffness of specimen,
- The third part, describing the plastic behavior of specimen.

For dynamic testing, Fourier transforms for specimen responses were plotted (figure-7) from which fundamental frequencies were deduced.

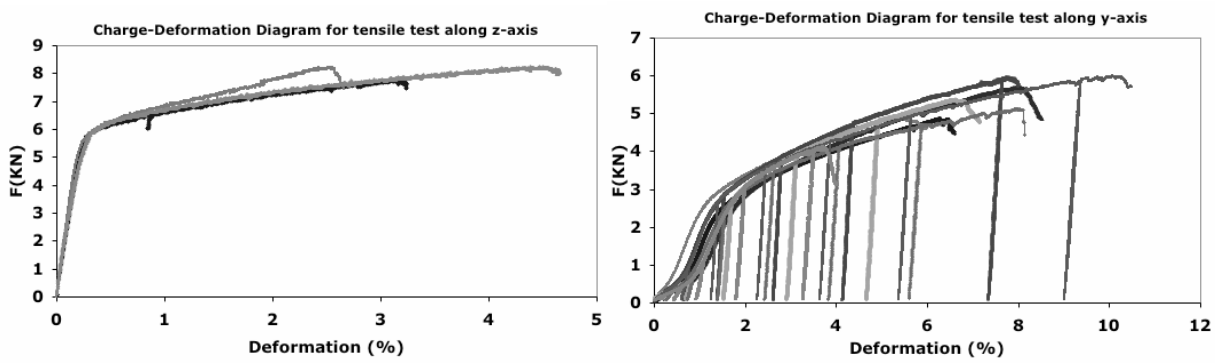

(a) (b)

Figure 6. Charge-Deformation diagrams of tensile tests (a) z-axis (b) y-axis

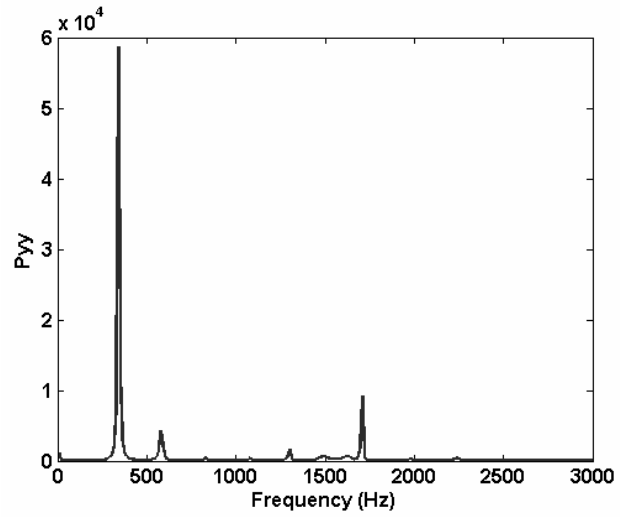

Figure 7. Fourier Transform of specimen response

Finite element calculation

Static and dynamic behaviors were in addition evaluated via finite element simulations. The stiffness matrix was found by modeling the RVE. Shell-type elements were used and six boundary condition cases were applied: 3 tractions and 3 shears. Tensile tests were also simulated. The behavior within the gauge length of specimens corresponding to the extensometer length was modeled. Boundary conditions for shear cases were inspired from Aitharaju and al. [2]. For dynamic behavior, 2 models were considered: a) homogenous model where specimens are considered as a homogeneous structure with an equivalent stiffness matrix found by static calculation and b) laminated model where specimens are considered being formed by stacking 2 plates each having equivalent orthotropic properties found by static calculation. Damping was not taken into account in calculation. A linear elastic calculation was performed and free vibration modes of specimens were computed. Figure 8 presents the different models used in simulations.

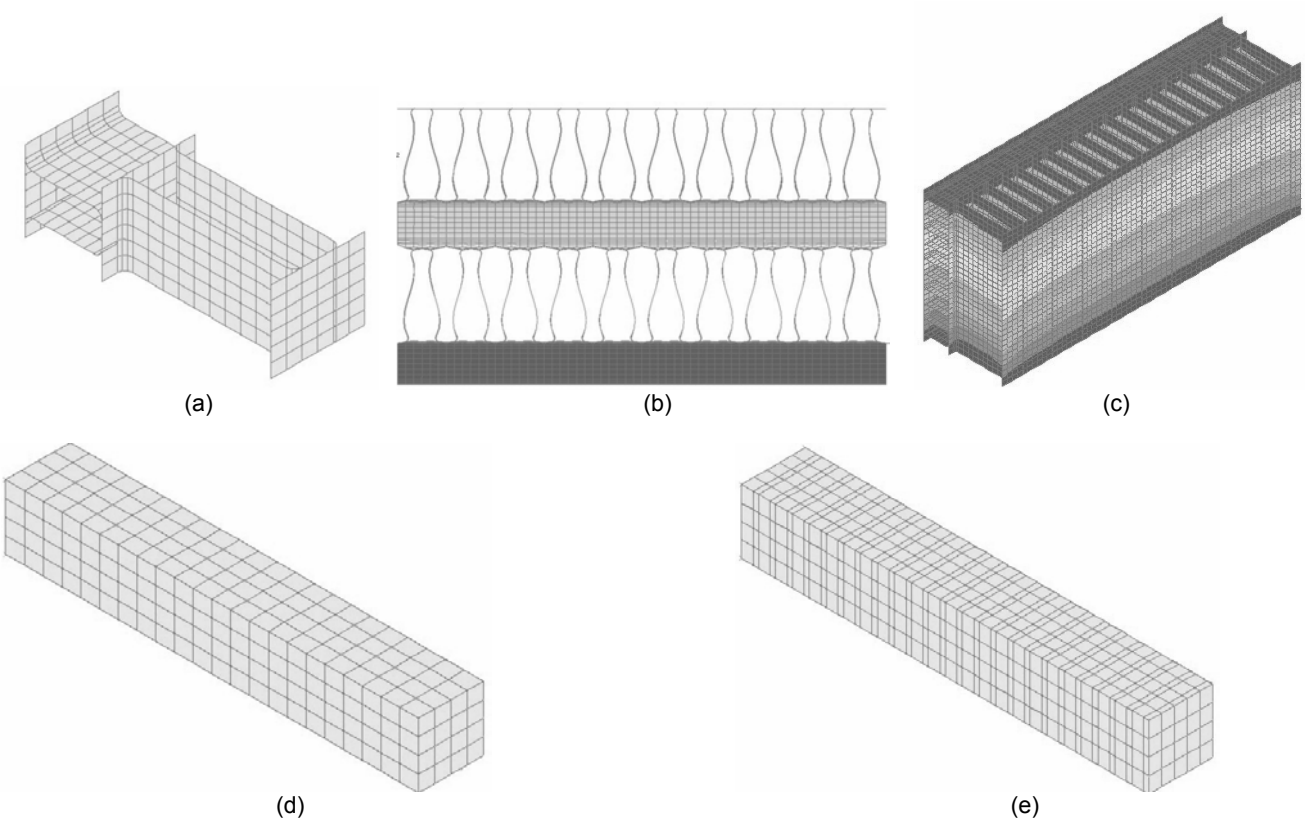

Figure 8. Different FM simulation approaches: (a) RVE of the core (b) Tensile test (y-axis) (c) Tensile test (z-axis) (d) Homogenous model for dynamic simulation (e) Laminated model for dynamic simulation

Results and discussion

Table 3 presents a comparison of tensile results along y and z directions.

Ky (KN/mm)				Kz (KN/mm)			
Experiment	Analytical	FEM	Variation (%)*	Experiment	Analytical	FEM	Variation (%)*
$121*10^{-3}*E$	$231.9*10^{-3}*E$	$129.2*10^{-3}*E$	47.8	1.59*E	1.44*E	1.63*E	9.4

Table 3. Average stiffness values for tensile specimens
*maximum variation between analytical and FEM with respect to experiment

A large variation is noticed between analytical and experimental stiffness values along y-direction. Finite element simulations on reduced models show that this variation might be due to stiffness variation between RVE's. In fact, the stiffness of RVE's varies according to their position in the structure. Therefore, a new analytical/numerical approach is proposed taking into consideration the presence of different types of boundary conditions on RVE's. Consider a substructure formed by assembling many RVE's in all three directions. RVE's can be classified into three types subjected to different boundary conditions (figure 9):

- Type 1: elements bounded from all sides by other RVE's,
- Type 2: elements forming the upper and lower face of the structure,
- Type 3: elements forming the rest of the structure.

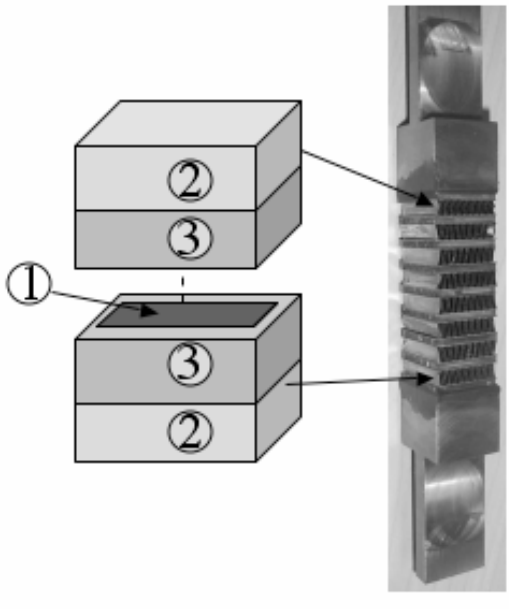

Figure 9. Classification of RVE's according to boundary conditions

To find the stiffness of each type of elements, different substructures are considered and finite element simulations are performed to find the average stiffness of substructures. In parallel, the stiffness of every substructure is expressed analytically in terms of the stiffness of each type of elements. A linear system of equations is obtained by this method. Stiffness of different types of elements is found by solving the system of equations. A new comparison of results is presented in table 4.

Ky (KN/mm)		
Experiment	Analytical/Numerical	Variation (%)*
$121*10^{-3}*E$	$125.6*10^{-3}*E$	3.66

Table 4. Average stiffness values along y-direction

Results show the efficiency of the new method.

Shear and dynamic results are presented in table 5 and figure 9 respectively.

	Gyz (Gpa)		Gxz (Gpa)	
	FEM	Analytical	FEM	Analytical
Unit cell 1	$35.62*10^{-3}*G$	$(33.13\text{-}39.34)*10^{-3}*G$	$23.40*10^{-3}*G$	$(24.48\text{-}31.97)*10^{-3}*G$
Unit cell 2	$42.65*10^{-3}*G$	$(31.95\text{-}42.36)*10^{-3}*G$	$52*10^{-3}*G$	$(55.66\text{-}67.82)*10^{-3}*G$

Table 5. Equivalent shear moduli for unit cells

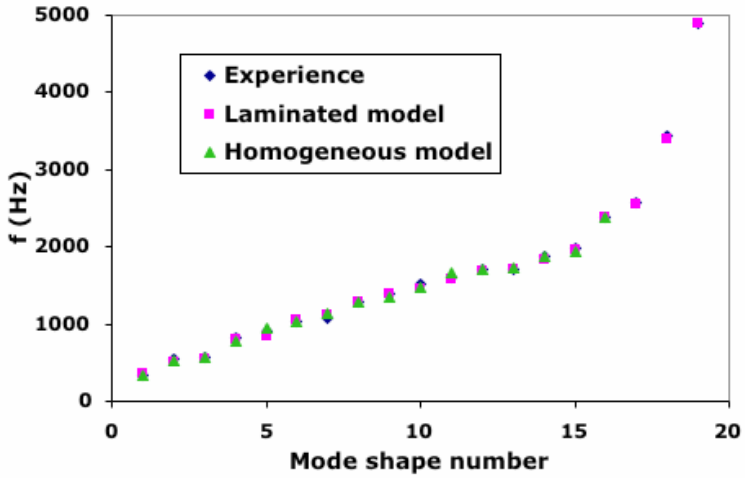

Figure 9. Comparison of fundamental frequencies between experience and the 2 F.E models

Regarding shear results, F.E values are within or very close to analytical limits. Since the objective of the present study is to find the equivalent stiffness matrix of the core, in order to further determine the static and dynamic behavior of the whole equipment, the small variations between results seem very satisfactory.
Concerning dynamic study, both homogenous and laminated models seem efficient in predicting fundamental frequencies of the structure. The homogeneous model requires fewer elements than the laminated model since the maximum size of elements for the latter is limited to the thickness of each ply. Consequently, the homogeneous calculation is less time-consuming approach. However, results of homogeneous model are limited to low frequencies. These models will be further submitted to thermal gradients to simulate the exchanger behavior in real service conditions.

Summary

The objective of the present study is to find the equivalent stiffness matrix of the core, in order to further determine the static and dynamic behavior of the whole equipment. Both analytical and FE calculations are employed to estimate the shear moduli and stiffness of the complex structure. Shear moduli are found estimated by an energy-based approach. Average in-plane stiffness is found via a spring-network method. Average out-of-plane stiffness is found by an analytical/numerical approach. It is observed that that the analytical and FEM approaches result in comparative achievement in terms of the estimations of the structural mechanical properties and behavior. The tensile and dynamic experiments are used for achieving the general behavior of 3D periodic structure.

Acknowledgment

The authors would like to thank Dr. D. Lucazeau for his valuable contribution.

References

1. Scida D., Aboura Z., Benzaggagh M.L., nad Bocherens E., “A micromechanics model for 3D elasticity and failure of woven-fibre composite materials”, Composite Science and Technology, 59, 1999, pp. 505-517.
2. Naik N.K. and Ganesh V.K., “An analytical method for plain weave fabric composites”, Composites, 26, 1995, pp. 281-289.
3. Aboura Z., Talbi N., Allaoui S. and Benzeggagh M.L., “Elastic behavior of corrugated cardboard: experiments and modeling”, Composite Structures, 63, 2004, pp. 53-62.
4. Aitharaju V.R. and Averill R.C., “Three-dimensional properties of woven-fabric composites”, Composites Science and Technology, 59, 1999, pp. 1901-1911.
5. Hohe J. and Becker W., “A refined analysis of the effective elasticity tensor for general cellular sandwich cores”, International Journal of Solids and Structures, 38, 2001, pp. 3689-3717.
6. Davalos J.F., Qiao P., Xu X.F., Robinson J. and Barth K.E., “Modeling and characterization of fiber-reinforced plastic honeycomb sandwich panels for highway bridge applications”, Composite Structures, 52, 2001, pp.441-452.
7. Ostoja-Starzewski M., Sheng P.Y. and Alzebdeh K., “Spring network models in elasticity and fracture of composites and polycrystals”, Computational Material Science, 7, 1996, pp. 82-93.